



# Long-term follow-up of a patient with *JAG1*-associated retinopathy

Muhammad R. Cheema · Lydia G. Stone · Peter W. Sellar · Stephanie Quinn · Stephen C. Clark · Richard J. Martin · Jill M. O'Brien · Clare Warriner · Andrew C. Browning 

Received: 6 January 2021 / Accepted: 2 April 2021  
© Crown 2021

## Abstract

**Purpose** To report the long-term structural and functional changes in the posterior segments of an adult with an unusual retinal dystrophy caused by a novel mutation in *JAG1*.

**Methods** A 33-year-old female underwent comprehensive ophthalmic examination, including best corrected visual acuity (BCVA) measurement, dilated fundus imaging (wide-angle fundus colour and short wavelength autofluorescence imaging), macular and peripheral spectral-domain optical coherence tomography (SD-OCT) and electroretinography (ERG) at baseline and 10 years later at the age of 43. The patient also underwent systemic review with detailed cardiac, brain and renal investigations. During follow-up, genetic analysis using whole-exome sequencing was performed on the patient and her parents to identify disease-causing variants.

**Results** The patient's main complaint was of a recent onset of bilateral photophobia and blurred vision in the left eye. On examination, the most striking retinal finding was of bilateral well-demarcated, anterior circumferential chorioretinal atrophy with scattered pigment clumping from the mid periphery to the ora. In addition, she had posterior pole RPE hypopigmentation, peripapillary chorioretinal atrophy, left macular choroidal folds and retinal vasculature tortuosity with atypical branching. Her retinal electrophysiology was consistent with a cone rod photoreceptor dystrophy and left macular dysfunction. Ten years later, her BCVA, the anterior circumferential chorioretinal atrophy and her visual field constriction all remained stable. Her retinal electrophysiology demonstrated deterioration of left rod function, while cone dysfunction remained stable. Macular function deteriorated in both eyes. During follow-up, she was also noted to

---

M. R. Cheema · L. G. Stone · A. C. Browning (✉)  
Newcastle Eye Centre, Royal Victoria Infirmary, Queen Victoria Road, Newcastle upon Tyne NE1 4LP, UK  
e-mail: andrew.browning@nhs.net

P. W. Sellar  
Ophthalmology Department, West Cumberland Hospital, Whitehaven CA28 8JG, Cumbria, UK

S. Quinn · C. Warriner  
Medical Physics Department, Royal Victoria Infirmary, Queen Victoria Road, Newcastle upon Tyne NE1 4LP, UK

S. C. Clark  
Department of Cardiothoracic Surgery, Freeman Hospital, Newcastle upon Tyne NE7 7DN, UK

R. J. Martin  
Department of Clinical Genetics, International Centre for Life, Newcastle upon Tyne NE1 3BZ, UK

J. M. O'Brien  
Sunderland Eye Infirmary, Queen Alexandra Rd, Sunderland SR2 9HP, UK

have progressive aortic root dilatation, posterior embryotoxon and an x ray diagnosis of butterfly vertebrae. Whole-exome sequencing revealed a novel c.2412C > A p.(Tyr804Ter) truncating mutation in *JAG1* that was predicted to be pathogenic and suggested a diagnosis of Alagille syndrome.

**Conclusion** This is the first report of the long-term detailed follow-up of a patient with Alagille syndrome whose most striking ophthalmic finding was bilateral well-demarcated, anterior circumferential chorioretinal atrophy. During follow-up, this finding remained stable, suggesting that this may be developmental in origin. This is in contrast with the progressive deterioration in the posterior pole retinal and macular function.

**Keywords** JAG1 · Electrophysiology · Sequencing

## Introduction

Mutations in *JAG 1* are associated with Alagille syndrome (OMIM 118450) and familial exudative vitreoretinopathy (FEVR) [1–3]. Alagille syndrome (ALGS) is a rare, autosomal dominant, multi-system disorder with an estimated incidence of 1:70,000 live births [4], which prior to the causative gene being identified, was diagnosed in patients by a histological paucity of intrahepatic bile ducts seen on a liver biopsy in combination with cholestatic jaundice and abnormalities in cardiac, vascular (most commonly peripheral pulmonary hypertension), ocular and skeletal (most commonly butterfly vertebrae) systems along with characteristic facial features [1, 5, 6]. Since the discovery that *JAG1* mutations cause the vast majority of cases [7], research has shown that the disease has poor phenotype genotype correlation [8] and that mutations can exhibit low penetrance and highly variable expression [9]. This has led to the recognition of a wide spectrum of additional features and mild disease phenotypes in ALGS [10, 11]. In the developing human eye, the expression of *JAG1* is greatest in the ciliary body, iris, lens and the anterior retina [12] which may explain why the most common ocular findings in ALGS are posterior embryotoxon and iris abnormalities [13]. It is also recognised that the posterior segment is also commonly involved in ALGS, with anomalous optic discs, retinal pigmentary

changes and maculopathy being seen in up to 76% of patients [13]. While the visual acuity of young patients with ALGS is reported as good, in the range of 6/12–6/18 [13], there is little long-term follow-up to determine whether the visual acuity remains stable and whether the retinal findings in particular are progressive.

We present the long-term clinical, multimodal imaging and electrophysiological follow-up of a previously well adult referred at the age of 33 with photophobia and the unusual retinal finding of bilateral, well-demarcated, anterior circumferential chorioretinal atrophy, who was subsequently found to have ALGS after a pathogenic *JAG1* mutation was discovered.

## Methods

### Clinical study

The medical records, multimodal retinal imaging and retinal electrophysiology studies of the patient were retrospectively reviewed. Ophthalmic examination including best corrected visual acuity measurement (BCVA), Goldmann perimetry, anterior segment slit lamp examination, dilated indirect funduscopy, wide-angle colour fundus and autofluorescence imaging (Optos plc, Dunfermline, UK) and macular optical coherence tomography (OCT) conducted using with manufacturer's retest function (Spectralis, Heidelberg, Germany) were reviewed. The sub-foveal choroidal thickness was measured as previously described [14]. The full-field electroretinogram (ERG), pattern electroretinogram (PERG) and the electrooculogram (EOG) were undertaken in accordance with the appropriate protocols of the International Society for Clinical Electrophysiology of Vision. (ISCEV) [15–18]. The results of the retinal electrophysiology were compared with laboratory generated, age-matched normal ranges. Systemic involvement was assessed by reviewing the patient's general medical records. The local research ethics committee declared that the work fell outside of the scope of Governance Arrangements for Research Ethics Committees 2020 section 2.3.1 and so therefore did not require prior ethics approval. The patient gave written informed consent for her case to be published and the work adhered to the tenets of the declaration of Helsinki.

## Molecular genetic study

At the first visit, a blood sample was collected from the patient; the DNA was extracted from peripheral lymphocytes and sent for a targeted NGS panel of 176 different genes including those known to be associated with retinitis pigmentosa and cone rod dystrophy. This was followed later by another blood sample taken from the patient, as well as both parents. This time the samples were sent to researchers coordinating the Deciphering Developmental Disorders (DDD) study. Copy number analysis and exome-based sequencing were performed via this study as previously described [19–21]. Data were filtered to look specifically for de novo variants in the coding or splicing sequences of the proband.

## Results

The patient was born at term from a normal pregnancy. There was no history of prematurity, post-natal jaundice, failure to thrive, short stature, hearing difficulties or lung disease. As a child, she was noted to have a cardiac murmur and mild learning difficulties. The murmur was subsequently diagnosed as an atrial septal defect, but closure was not required. As an adult, she was diagnosed with hyperthyroidism at the age of 22, which was treated by sub-total thyroidectomy. At the age of 24, she visited an optometrist complaining of flashing lights and floaters. Her BCVA was recorded as 6/7.5 bilaterally, her refraction was OD  $-8.75/-0.5 \times 40$  and OS  $-8.5/-1.5 \times 130$ , and fundoscopy showed bilateral peripheral chorioretinal atrophy. At the age of 33, the patient was referred to this institution with a long history of photophobia, an 18-month history of reduced vision in the left eye and a strange appearance of the peripheral retina in both eyes. The patient denied any symptoms of nyctalopia. Her BCVA was OD 6/12 ( $-8.5/-0.5@90$ ) and OS 6/18 ( $-2.25/-1.5@130$ ), and her Goldmann visual field (GVF) examination demonstrated concentric visual field constriction in both eyes (Fig. 1). Anterior segment slit lamp examination demonstrated bilateral posterior embryotoxon and dilated fundoscopy revealed mild posterior sub-capsular cataracts (lenses were of normal morphology), posterior pole RPE hypopigmentation, peripapillary chorioretinal atrophy, left macular choroidal folds, retinal vasculature

tortuosity with atypical branching and most strikingly, bilateral, well-demarcated, circumferential peripheral chorioretinal atrophy with scattered pigment clumping from the mid periphery to the ora (Fig. 2). Wide-angle autofluorescence imaging demonstrated well-demarcated, bilateral peripheral hypoautofluorescence which coincided with the circumferential chorioretinal atrophy. In addition, there was a thin hyperautofluorescent band at the posterior edge of the circumferential chorioretinal atrophy (Fig. 2). Both optic discs had a normal appearance with normal retinal nerve fibre layer thicknesses on disc OCT scans. A macular OCT scan of the right eye was unremarkable with an intact ellipsoid zone and a sub-foveal choroidal thickness (SFCT) of 161  $\mu\text{m}$ , while the left showed marked chorioretinal folds and disruption of some areas of the ellipsoid zone and a SFCT of 222  $\mu\text{m}$  (Fig. 3). The reference range for SFCT in normal eyes is reported to be 250–350  $\mu\text{m}$  [22]. Macular fundus autofluorescence of the right eye was normal whereas the left demonstrated horizontal lines of hyperautofluorescence corresponding with the chorioretinal folds (Fig. 3). Peripheral OCT scans demonstrated that the loss of the photoreceptor layer corresponded with the posterior junction of the circumferential chorioretinal atrophy (Fig. 4). Fundus fluorescein angiography showed that some of the peripheral retinal vessels crossed the posterior edge of the circumferential chorioretinal atrophy but otherwise added no additional information. An MRI of the brain and orbits performed to investigate the cause of the chorioretinal folds revealed no evidence of extra ocular compression or extraocular muscle abnormalities. The optic nerves had a normal appearance; however, it was commented on that the globes appeared deformed, more marked on the left, which was confirmed on ultrasound B scan with both posterior segments having a conical shape with posterior pole flattening. (Fig. 5) There was no evidence of optic disc drusen or posterior staphyloma on ultrasound B scans. Interestingly, despite the patient having a myopic refraction, her axial lengths were OD 23.2 mm and OS 21.5 mm. Keratometry showed that both corneas were very steep (OD K1 = 48.1D, K2 = 48.8D and OS K1 = 47.8D, K2 = 48.7D). The mean corneal power of adult patients with normal axial lengths (22–24.5 mm) is reported to be  $44.37 \pm 1.39\text{D}$  [23].

Retinal electrophysiology performed at the age of 33 demonstrated results in keeping with a cone rod

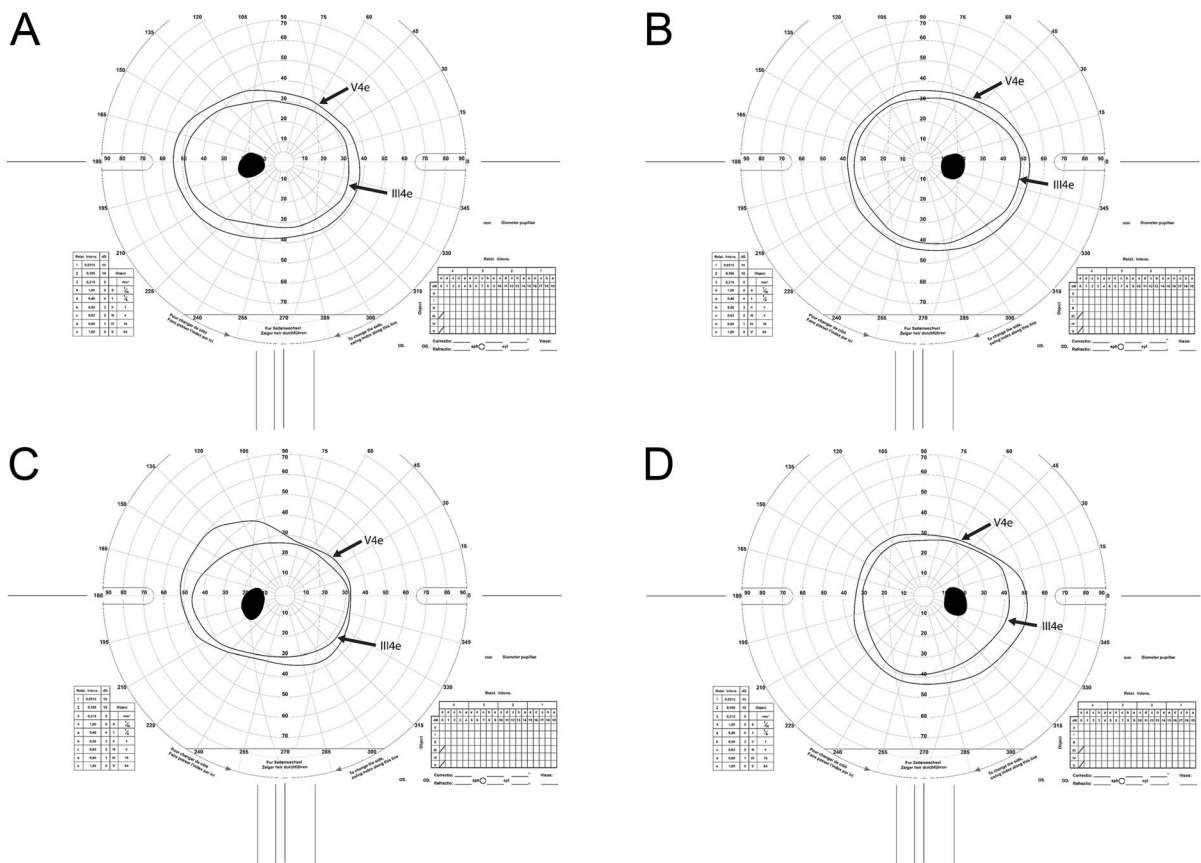


**Fig. 1** Goldman visual fields of the patient's left (A) and right eyes (B) at age 33 and the left (C) and right (D) eyes age 43. The bilateral concentric visual field constriction remains generally stable over the 10 years of follow-up

dystrophy with the dark adapted rod specific (DA 0.01) responses being borderline attenuated, while the DA 3.0 ERG (mixed rod/cone) a and b wave responses, the light adapted (LA 3.0) single flash a and b waves and the 30 Hz flicker cone ERG b waves were all attenuated (Fig. 6). All peak times were within normal limits. The pattern ERG of the right eye was within normal limits; however, the left was markedly attenuated indicating left macular dysfunction. The EOG was Arden ratio was 1.9 OU. These results would explain the patient's photophobia (cone dysfunction) and blurred left vision (macular dysfunction). The patient's plasma ornithine level was 109  $\mu\text{mol/l}$  (reference range 30–150), and analysis of the targeted NGS panel of 176 retinal genes was unremarkable except for a heterozygous mutations in *MYO7A* (c397C > A) and *CFAP410* (c218G > C). The first mutation has previously been reported in a patient with Ushers syndrome type 1B, who was

compound heterozygous with a second missense change [24]; however, our patient had no other clinical features to suggest a diagnosis of type 1B Usher's syndrome. The second mutation has previously been reported in a biallelic state in a patient with axial spondylometaphysial dysplasia and retinitis pigmentosa [25] A limited number of other conditions may have a similar retinal phenotype, but no pathogenic mutations were detected in *BEST1* or *OAT* and the patient's EOG and plasma ornithine level were both normal, making the diagnosis of autosomal dominant vitreoretinopathy (ADVIRC) and gyrate atrophy extremely unlikely At this point, the cause of the patient's retinal dystrophy remained unknown.

At the age of 41, she was investigated for difficult to control hypertension. Echocardiography and a CT angiogram demonstrated mild aortic regurgitation through a tricuspid aortic valve and significant aortic root dilatation (4.5 cm). The ascending aorta was of

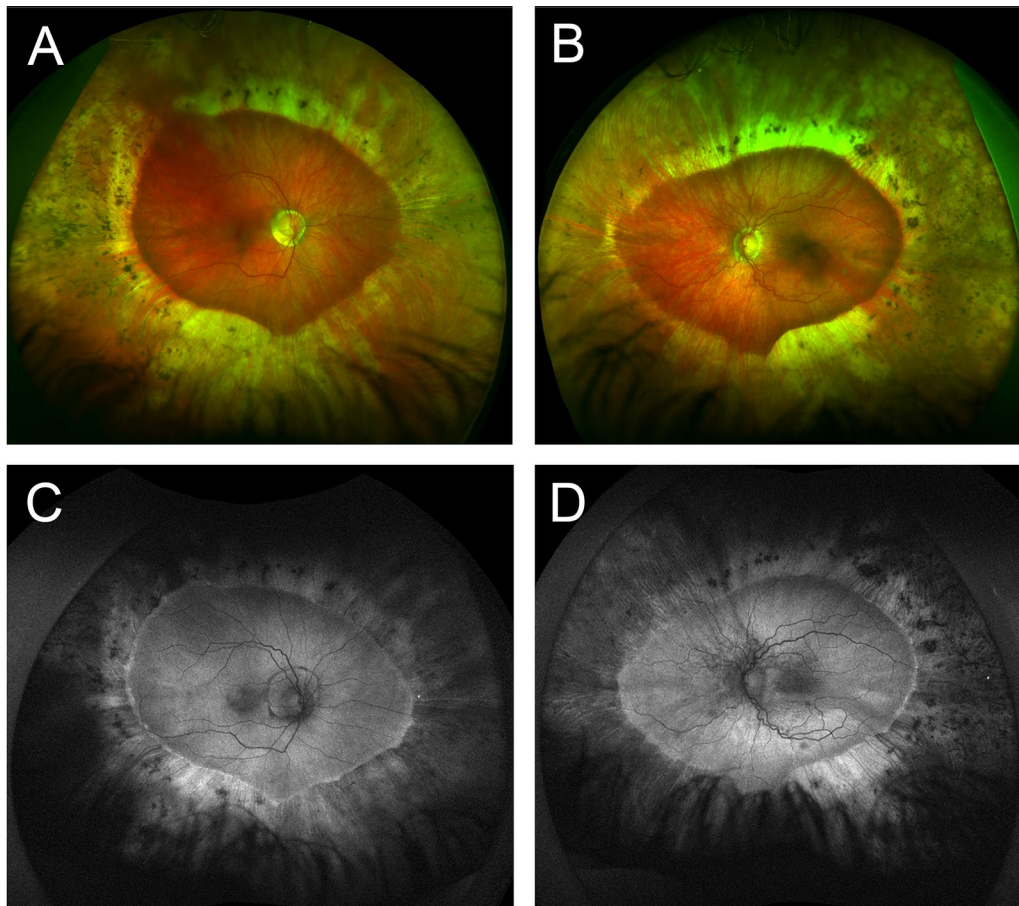


**Fig. 2** Wide-angle colour fundus images of the right (A) and left (B) eyes and short wavelength fundus autofluorescence images of the right (C) and left (D) eyes at age 33. These demonstrate posterior pole RPE hypopigmentation, peripapillary chorioretinal atrophy, retinal vasculature tortuosity with

normal calibre and there was no evidence of renal artery stenosis. There were no abnormalities of the pulmonary valve and no evidence of pulmonary hypertension. Given her cardiac findings and her height (172 cm), it was suspected that she may have Marfan's syndrome; however, *FBN1* gene testing was negative. As an incidental finding, her CT thorax demonstrated unfused or butterfly vertebrae at T3, T7 and T10.

Subsequent whole-exome sequencing revealed a novel c.2412C > A p. (Tyr804Ter) truncating mutation in exon 20 of *JAG1*. Neither of the patient's parents carried the mutation, indicating that it was de novo. In silico analysis predicted this mutation to be truncating and therefore pathogenic and suggested of a

atypical branching, and most strikingly, bilateral, well-demarcated, circumferential chorioretinal atrophy with scattered pigment clumping from the mid periphery to the ora. The fundus autofluorescence images show a hyperautofluorescent band at the margin of the peripheral atrophy

diagnosis of Alagille syndrome. This prompted further investigations which included an abdominal ultrasound scan (normal kidney, liver and gall bladder structure) and blood tests (normal full blood count, renal and liver function, with no indication of cholestasis). Her facial features showed her to have a broad forehead, deep set eyes and a pointed, bulbous chin which is keeping with ALGS. Examination revealed that her hands and feet were normal.

When the patient underwent ophthalmic review at the age of 43, she had received bilateral cataract surgery at a different institution and she felt that her vision was stable. She continued to complain of photophobia and again denied any nyctalopia. Her BCVA was recorded as OD 6/15 and OS 6/18, and

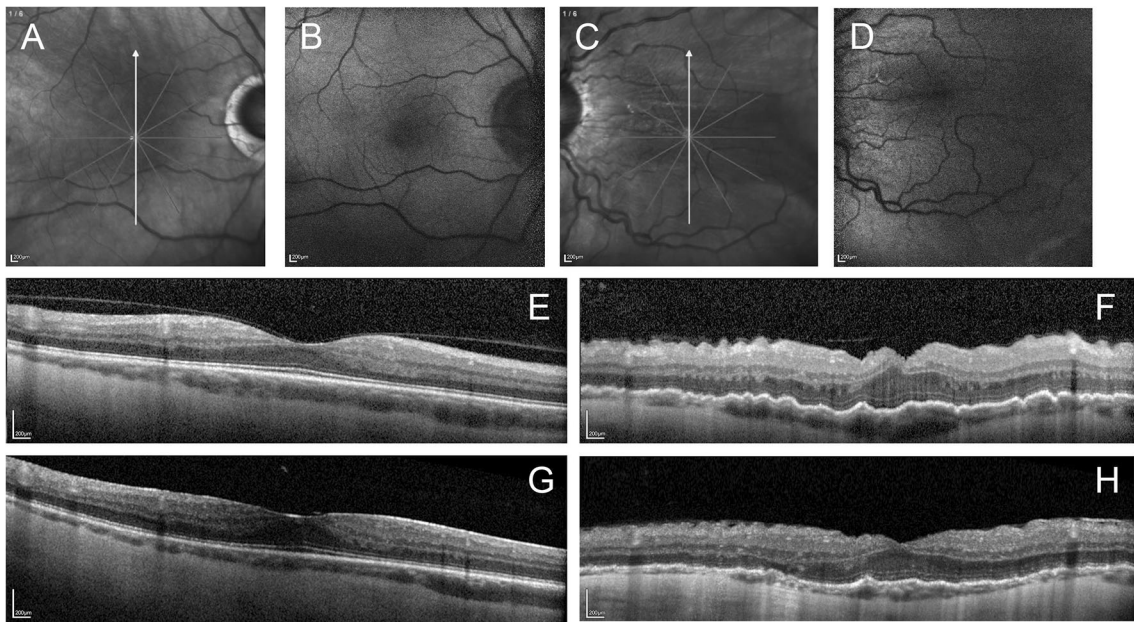


**Fig. 3** Infrared reflectance (A, C) and fundus autofluorescence (B, D) images of the right and left eyes, respectively (age 33). The vertical white lines on the infrared reflectance images correspond to the location of the macular OCT line scans. Images E and G represent SD OCT line scans through the right macula at ages 33 and 43, respectively. Both images demonstrate normal macular morphology and an intact EZ. It can be

seen that there has been some choroidal thinning during the 10 years of follow-up. Images F and H represent SD OCT line scans through the left macula at ages 33 and 43, respectively. Image F demonstrates marked chorioretinal folds and disruption of the EZ across the macula. Ten years later, image H shows that the chorioretinal folds have markedly improved; however, there has been significant choroidal thinning

GVF examination showed no significant change in visual field constriction (Fig. 1).

Comparison with the macular OCT scans recorded 10 years previously, showing that the EZ remained well-preserved OD and disrupted OS (Fig. 3). Interestingly, the left choroidal folds had markedly improved. It was also noted that choroidal thinning had occurred in both maculae over the 10 years (SFCT = 97  $\mu\text{m}$  OD and 113  $\mu\text{m}$  OS at age 43) (Fig. 3). Careful examination of wide-angle retinal imaging showed minimal progression of the posterior edge of the circumferential CR atrophy. (Fig. 4); however, there was a significant reduction in DA 0.01 b wave and DA 3.0 a and b wave amplitudes in the left eye and a mild reduction in the right eye indicating a reduction in rod photoreceptor function while the worsening of the pattern ERG P50 components in both eyes suggested a deterioration in macular function bilaterally (Fig. 6). Cone photoreceptor dysfunction was stable. At her most recent cardiac review, surveillance by echocardiography and CT demonstrated progression to mild-moderate aortic valve

regurgitation and some enlargement of the Sinuses of Valsalva to 4.9 cm over the previous 2 years, although she remained completely asymptomatic. The ascending aorta remained of normal calibre.

## Discussion

In this report, we present the long-term follow-up of a 33-year-old female with an unusual retinal appearance and long-standing photophobia. Initial investigation excluded retinopathy of prematurity, gyrate atrophy and ADVIRC. Subsequent investigation found a novel pathogenic truncating mutation in the 15th EGF-like calcium binding domain of *JAG1* which prompted further ocular and systemic investigation. This led to the finding of a number of systemic features that suggested her unusual retinal changes were the initial presenting feature of ALGS. The most striking feature of the posterior segment was a well-demarcated, bilateral, anterior circumferential peripheral chorioretinal atrophy. On careful examination, she also had

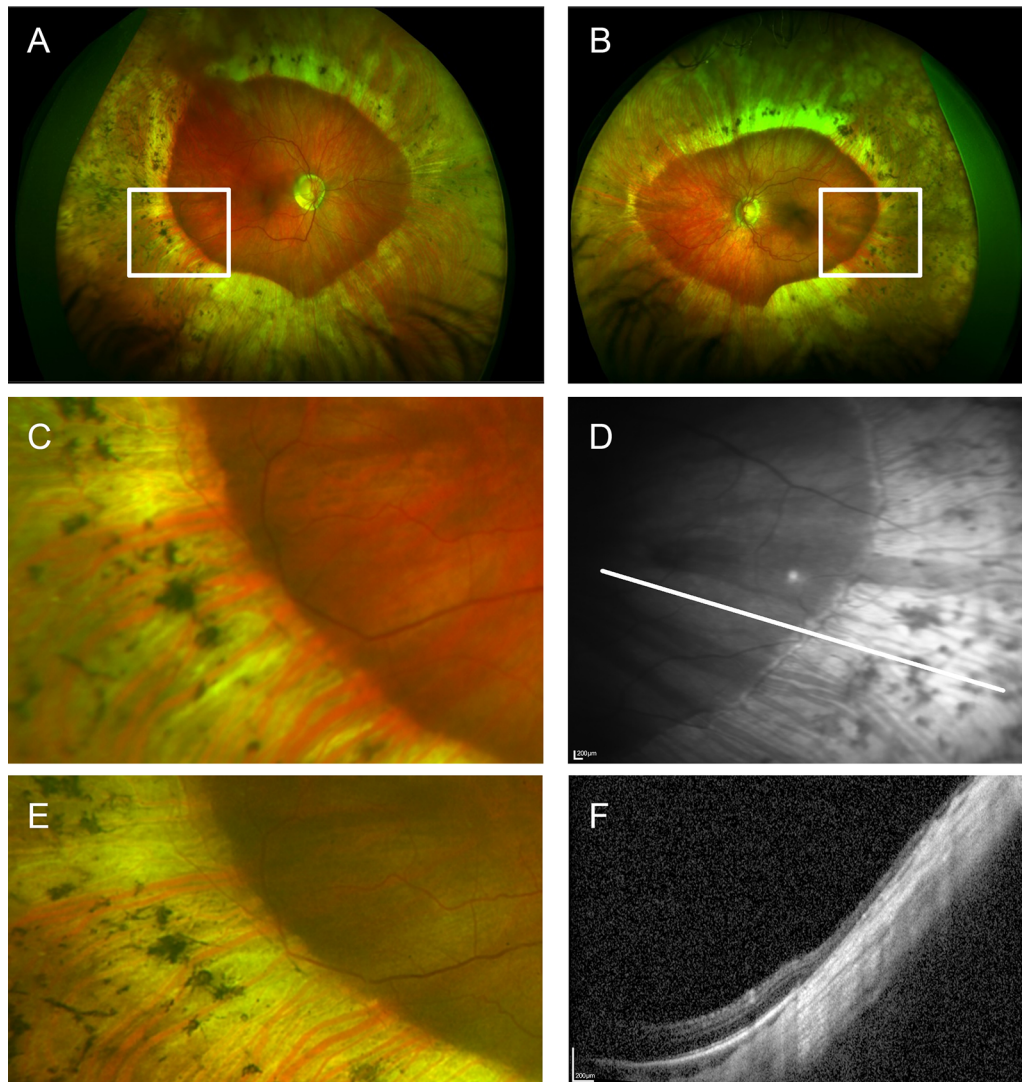


**Fig. 4** Wide-angle colour fundus images of the right (A) and left (B) eyes showing areas of interest within the white boxes. C and E show an area in the right eye (A) at ages 33 and 43, respectively. Using the visible retinal blood vessel as a guide, the posterior extension of the chorioretinal atrophy is minimal.

D Red free image of an area in the left eye (B). The oblique white line is the axis of SD OCT scan (F) which shows complete loss of outer retinal structure, starting at the junction of chorioretinal atrophy

diffuse posterior pole RPE hypopigmentation, unilateral macular choroidal folds, retinal vascular tortuosity and cone/rod dysfunction. Mutations in *JAG1* are found in up to 95% of ALGS [7], and to date, approximately 700 pathogenic mutations have been identified, scattered throughout the entire gene coding sequence with no apparent mutation hot spots and with no obvious genotype/phenotype correlation [26]. Approximately 70% of mutations are protein

truncating, with the majority being de novo [7, 11, 27]; Spinner et al. have suggested that as protein truncating variants and the less common whole gene deletions and intragenic pathogenic variants all have similar phenotypes, haploinsufficiency is the most likely disease causing mechanism [28]. While bile duct paucity and subsequent cholestasis are the most common findings (up to 94%) in “typical” ALGS [6], our patient had no history of early jaundice

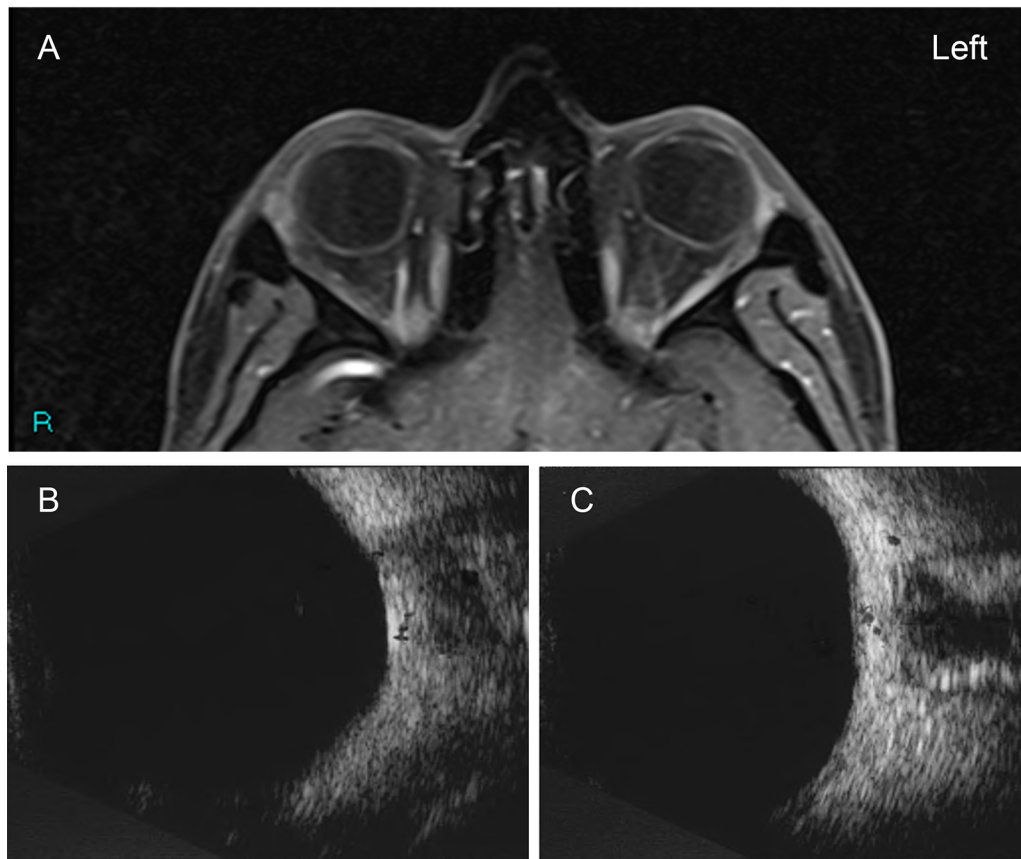


**Fig. 5** An axial T1 weighted MRI scan of the orbits showing the abnormal conically shaped and flattened posterior globes (A). These findings are confirmed by B scan ultrasound images through the optic nerves of the right (B) and left (C) globes

and her liver ultrasound and liver function blood tests were normal. Secondly, although abnormalities of the right side of the heart and peripheral pulmonary hypertension are the most common cardiovascular abnormalities seen in ALGS (up to 67%) [6], they were again absent in our case; however, she had recently been diagnosed with progressive dilation of the Sinuses of Valsalva, which has previously been reported in a very small number of patients with ALGS [29–31].

In the largest study to date, Hingorani et al. [13] reported a number of posterior segment changes that are associated with ALGS, including diffuse hypopigmentation of the RPE (57%), diffuse speckling or granularity of the RPE (33%), maculopathy (18%) and anomalous optic discs, which may include optic disc drusen (72%). The finding of anterior circumferential chorioretinal atrophy has been reported previously in a small number of mostly adult ALGS cases, although

one case was diagnosed post-mortem at 6 years of age [32–36]. In 2 of the cases, patients with anterior circumferential chorioretinal atrophy, the phenotype was complicated by bilateral macular atrophy in a face-mask configuration [32, 34] and when tested, all cases had normal visual fields and/or normal full-field ERGs. To date, no *JAG1* mutations have been reported in patients with this retinal phenotype.

Interestingly, a small number of patients with ALGS at different ages have undergone full-field ERGs and these demonstrated variable results with no clear correlation with retinal phenotype. Results ranged from normal rod and cone function, reduced rod function to no detectable retinal function [9, 33, 35, 37]. Prior to our case, only one patient has previously been reported to have predominantly reduced retinal cone function [35]. Like most cases, this patient had a pigmentary retinopathy, but unlike others, they also had macular disease and choroidal

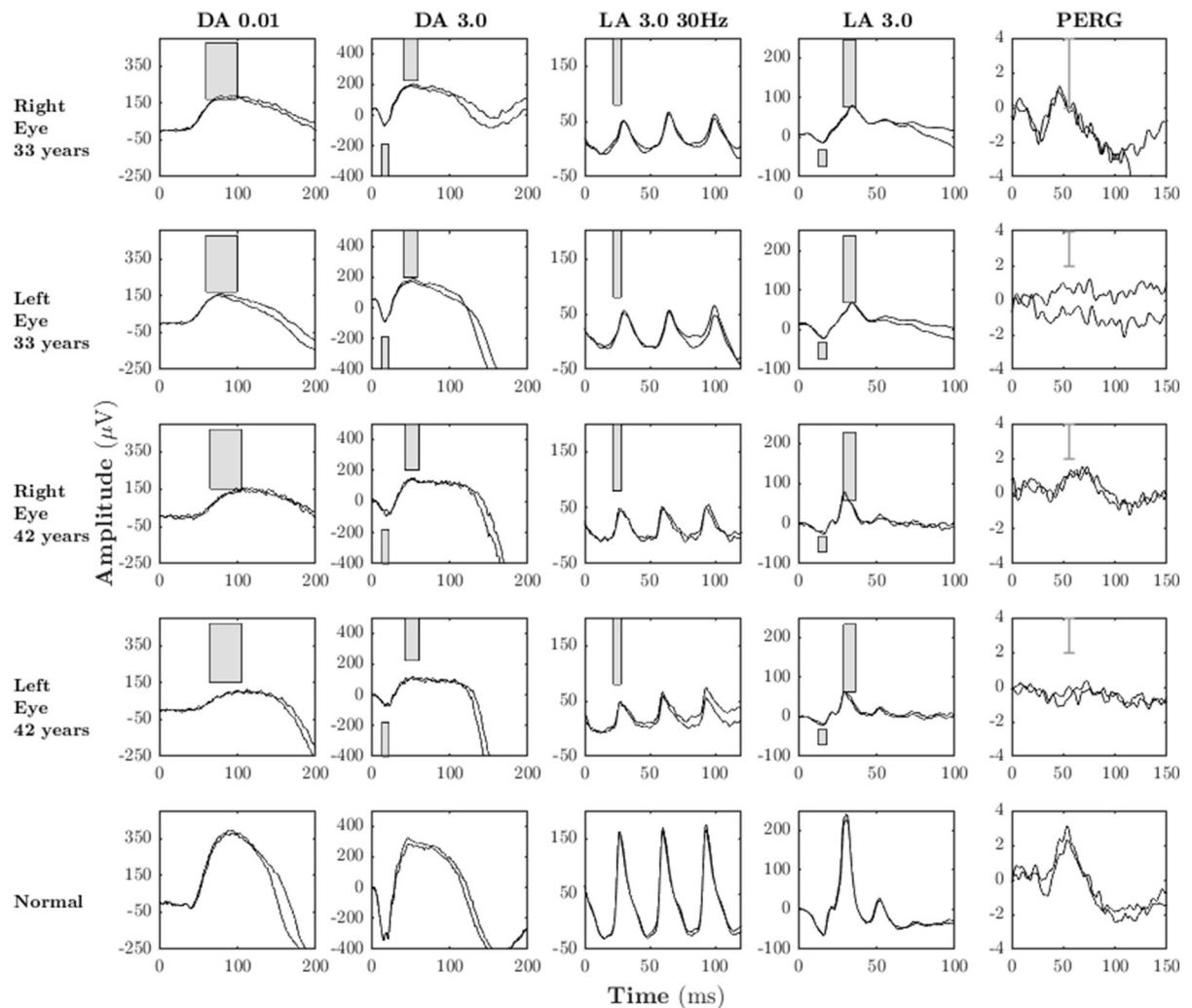


**Fig. 6** Full-field electroretinograms (ERG) and pattern electroretinograms (PERG) of the right and left eyes at ages 33 and 43. At the age of 33, the photopic responses are attenuated while the scotopic DA 0.01 responses are borderline attenuated. The DA 3.0 a and b wave responses are both attenuated bilaterally, probably reflecting the combined effect of the rod and cone dysfunction. The right PERG response is normal, whereas the

left is markedly attenuated. At the age of 43, the photopic responses remain attenuated but stable, whereas there has been a worsening scotopic response, predominantly at the level of the photoreceptor. This is most marked in the left eye. The PERG response has worsened in the right eye and remains markedly attenuated in the left. The grey boxes denote the laboratory-derived age-matched normal ranges for each response

folds. Unfortunately, many of these reports were historical in nature and the electrophysiology was often not performed to ISCEV standards and was not repeated to assess disease progression.

In agreement with most reported ALGS patients, the visual acuity of our case was only mildly affected and was stable over 10 years of follow-up. While Hingorani et al. found that in their cohort of 22 patients, the mean spherical equivalent was + 0.85D (range -2.25 to + 5.5) [13]; our case was myopic, albeit with normal/

slightly short axial lengths. Her corneas were very steep however, which would account for the majority of her myopia. Visual field, multimodal retinal imaging and retinal electrophysiology studies 10 years apart demonstrated little, if any, posterior progression of the peripheral circumferential changes or change of the concentric visual field constriction; however, retinal electrophysiology demonstrated progressive retinal and macular dysfunction. Peripheral OCT imaging of our patient and a previous example of histology

examination of an ALGS globe with peripheral anterior chorioretinal atrophy [36] both demonstrate severe outer retinal and RPE disruption anterior to the demarcation line, suggesting that worsening of retinal electrophysiological function is most likely due to deterioration in the area of retina affected by generalised RPE hypopigmentation in the posterior pole. Despite her visual acuity being stable, her pattern ERG demonstrated a marked decline in macular function particularly in her better seeing right eye, despite preservation of the macular EZ, which is thought to be a robust indicator of photoreceptor integrity. The sub-foveal choroidal thickness was sub-normal bilaterally at baseline, and interestingly, there was progressive thinning over the decade of follow-up with the right SFCT reducing by 64  $\mu\text{m}$  (40%) and the left by 109  $\mu\text{m}$  (49%). It has been reported that in myopic patients, SFCT decreases by 11.9  $\mu\text{m}$  per decade and is inversely correlated with visual acuity, so for our patient, this significant reduction in bilateral SFCT may be contributing to the deterioration of macular photoreceptor function [38].

There appears to be a dichotomy between the progressive nature of the well-recognised posterior pole structural and functional changes and the stable but uncommon peripheral findings. One explanation for this could be that in our patient, they are separate entities, both resulting from the *JAG1* mutation. It is possible that the stationary, peripheral changes may be developmental, based on the finding of high *JAG1* expression in the anterior retinae of human embryos [12], the phenotype being previously seen in a 6-year-old patient [36], the abnormally shaped globes on ocular ultrasound and the important role of *JAG1* in early peripheral retinal vascular development, as recently demonstrated by the finding of pathogenic mutations in *JAG1* being found in cases of FEVR [3]. In the future, it would be interesting to undertake wide-angle imaging of ALGS patients soon after birth to determine the rarity of anterior circumferential atrophy early in life and to perform long-term follow-up to ascertain disease progression and to establish if there is any genotype/phenotype correlation for this feature.

In conclusion, we present an adult with an unusual retinal dystrophy and long-standing photophobia, who was subsequently diagnosed with mild Alagille syndrome after a pathogenic mutation in *JAG1* was discovered. We show that in this patient, over a

10-year period, there was progressive retinal electrophysiological dysfunction; however, the unusual bilateral anterior circumferential atrophic changes were stationary.

**Funding** None.

**Availability of data and material** Available on request.

**Declarations**

**Conflict of interest** None.

**Ethics approval** The local research ethics committee declared that the work fell outside of the scope of Governance Arrangements for Research Ethics Committees 2020 section 2.3.1 and so therefore did not require prior ethics approval.

**Consent for publication** The patient gave written informed consent for her case to be published.

**Consent to participate** The patient gave written informed consent to participate in this work.

**Statement of human rights** All procedures performed on the study involving the human participant were in accordance with the ethical standards of the institutional and/or national research committee and with the 1964 Declaration of Helsinki and its later amendments or comparable ethical standards.

**Statement on the welfare of animals** This article does not contain any studies with animals.

**Informed consent** The patient gave written informed consent to participate in this study.

## References

- Li L, Krantz ID, Deng Y et al (1997) Alagille syndrome is caused by mutations in human Jagged1, which encodes a ligand for Notch1. *Nat Genet* 16:243–251
- Oda T, Elkahoulun AG, Pike BL et al (1997) Mutations in the human Jagged1 gene are responsible for Alagille syndrome. *Nat Genet* 16:235–242
- Zhang L, Zhang X, Xu H, Huang L, Zhang S, Liu W et al (2020) Exome sequencing revealed Notch ligand JAG1 as a novel candidate gene for familial exudative vitreo-retinopathy. *Genet Med* 22:77–84
- Danks DM, Campbell PE, Jack I, Rogers J, Smith AL (1977) Studies of the aetiology of neonatal hepatitis and biliary atresia. *Arch Dis Child* 52:360–367
- Alagille D, Estrada A, Hadchouel M, Gautier M (1987) Odieuvre M, Dommergues JP: syndromic paucity of interlobular bile ducts (Alagille syndrome or arteriohepatic dysplasia): review of 80 cases. *J Pediatr* 110:195–200
- Emerick KM, Rand EB, Goldmuntz E, Krantz ID, Spineer NB, Piccoli DA (1999) Features of Alagille syndrome in 92

- patients: frequency and relation to prognosis. *Hepatology* 29:822–829
7. Gilbert MA, Bauer RC, Rajagopalan R, Grochowski CM, Chao G, McEldrew D, Nassur JA et al (2019) Alagille syndrome mutation update syndrome: Comprehensive overview of JAG1 and NOTCH 2 mutation frequencies and insight into missense variant classification. *Hum Mutat* 40:2197–2220
  8. Krantz I, Colliton R, Genin A, Rand E, Li L, Piccoli D, Spinner N (1998) Spectrum and frequency of jagged1 (JAG1) mutations in Alagille syndrome patients and their families. *Am J Hum Genet* 62:1361–1369
  9. Kim BJ, Fulton AB (2007) The genetics and ocular findings of Alagille syndrome. *Semin Ophthalmol* 22:205–210
  10. Kamath BM, Bason L, Piccoli DA, Krantz ID, Spinner NB (2003) Consequences of JAG1 mutations. *Med Genet* 40:891–895
  11. Guegan K, Stalsa K, Daya M, Turnpenny P, Ellard S (2012) JAG1 mutations are found in approximately one third of patients presenting with only one or two clinical features of Alagille syndrome. *Clin Genet* 82:33–40
  12. Jones EA, Clement Jones M, Wilson DI (2000) *JAGGED1* expression in human embryos: correlation with Alagille syndrome phenotype. *J Med Genet* 37:658–662
  13. Hingorani M, Nischal KK, Davies A, Bentley C, Vivian A, Baker AJ (1999) Ocular abnormalities in Alagille syndrome. *Ophthalmology* 106:330–337
  14. Browning AC, O'Brien JM, Vieira RV, Gupta R, Nenova K (2019) Intravitreal Aflibercept for retinal angiomatous proliferation: Results of a prospective case series at 96 weeks. *Ophthalmologica* 242:239–246
  15. Marmor MF, Fulton AB, Holder GE, Miyaki Y, Brigell M, Bach M (2004) Standard for clinical electroretinography (2008 update). *Doc Ophthalmol* 118:69–77
  16. McCulloch DL, Marmor MF, Brigell MG, Hamilton R, Holder GE, Tzekov R (2015) BachM ISCEV Standard for full-field clinical electroretinography (2015 update). *Doc Ophthalmol* 130:1–12
  17. Brown M, Marmor M, Vaegan, Zrenner E, Brigell M, Bach M (2006) ISCEV standard for clinical electro-oculography (EOG) 2006. Brown M, et al. *Doc Ophthalmol*; 113(3):205–12
  18. Bach M, Brigell MG, Hawlina M, Holder GE, Johnson MA, McCulloch DL et al (2013) ISCEV standard for clinical pattern electroretinography (PERG): 2012 update *Doc. Ophthalmol* 126:1–7
  19. Deciphering Developmental Disorders study (2015) Large scale discovery of novel genetic causes of developmental disorders. *Nature* 519(7542):223–228
  20. Firth HV, Wright CF (2011) The deciphering Developmental Disorders (DDD) study. *Dev Med Child Neurol* 53:702–703
  21. Wright CF, Fitzgerald TW, Jones WD, Clayton S, McRae JF, van Kogelenberg M et al (2015) Genetic diagnosis of developmental disorders in the DDD study: a scalable analysis of genome wide research data. *Lancet* 385(9975):1305–1314
  22. Kong M, Choi DY, Han G, Song YM, Park SY, Sung J et al (2018) Measurable range of Subfoveal choroidal thickness with conventional spectral domain optical coherence tomography. *Transl Vis Sci Technol* 7:16
  23. Yu J, Zhong J, Mei Z, Zhao F, Tao N, Xiang Y (2017) Evaluation of biometry and corneal astigmatism in cataract surgery patients from central China. *BMC Ophthalmol* 17:56
  24. Roux AF, Faugère V, Le Guédard S, Pallares-Ruiz N, Vielle A, Chambert S et al (2006) Survey of the frequency of USH1 gene mutations in a cohort of Usher patients shows the importance of cadherin 23 and protocadherin 15 genes and establishes a detection rate of above 90%. *J Med Genet* 43:763–768
  25. Wang Z, Lida A, Miyake N, Nishiguchi KM, Fujita K, Nakazawa T et al (2016) Axial spondylometaphyseal dysplasia is caused by c21orf2 mutations. *PLoS ONE* 11(3):e0150555
  26. Turnpenny PD, Ellard S (2012) Alagille syndrome: pathogenesis, diagnosis and management. *Eur J Hum Genet* 20:251–257
  27. Crosnier C, Driancourt C, Raynaud N et al (1999) Mutations in *JAGGED1* gene are predominantly sporadic in Alagille syndrome. *Gastroenterology* 116:1141–1148
  28. Spinner NB, Colliton RP, Crosnier C, Krantz IC, Hadchouel M, Meunier-Rotival M (2001) Jagged1 mutations in Alagille syndrome. *Hum Mutat* 17:18–33
  29. Kamath BM, Spinner NB, Emerick KM, Chudley AE, Booth C, Piccoli DA et al (2004) Vascular anomalies in alagille syndrome a significant cause of morbidity and mortality. *Circulation* 109:1354–1358
  30. Molinero-Herguedas E, Labrador-Fusteret T, Rios-Lazaro M, Carmaniu-Tobal J (2008) Aortic aneurysm in alagille syndrome. *Rev Esp Cardiol* 61:653–659
  31. Smithson S, Hall D, Trachtenberg B, Bhimaraj A, Estep JD, Balzer DT et al (2014) Treatment of cardiovascular complications of Alagille syndrome in clinical optimisation for liver transplantation. *Int journal cardiolo* 176:e37–e40
  32. Esmaili DD (2015) Chorioretinal atrophy in Alagille syndrome. *Retin Cases Brief Rep* 9:330–332
  33. Puklin JE, Riely CA, Simon RM, Cotlier E (1981) Anterior segment and retinal pigmentary abnormalities in arteriohepatic dysplasia. *Ophthalmology* 88:337–347
  34. Makino S (2016) Tampo H peripheral circumferential chorioretinal atrophy in a patient with alagille syndrome. *Imaging J Clin Med Sci* 3:009–009. <https://doi.org/10.17352/2455-8702.000026>
  35. Wells KK, Pulido JS, Judisch GF et al (1993) Ophthalmic features of Alagille syndrome (arteriohepatic dysplasia). *J Pediatr Ophthalmol Strabismus* 30:130–135
  36. Johnson BL (1990) Ocular pathologic features of arteriohepatic dysplasia (Alagille's syndrome). *Am J Ophthalmol* 110:504–512
  37. Tanino T, Ishihara A, Naganuma K et al (1986) Electrophysiological findings in a family with congenital arteriohepatic dysplasia (Alagille syndrome). *Doc Ophthalmol* 63:83–89
  38. Ho M, Liu DT, Chan VCK, Lam DSC (2013) Choroidal thickness measurement in myopic eyes by enhanced depth optical coherence tomography. *Ophthalmology* 120:1909–1914